34th Annual International Conference of the IEEE EMBS
San Diego, California USA, 28 August - 1 September, 2012

Implantable Ultrasonic Dual Functional Assembly for Detection and Treatment of Anomalous Growth

Abhishek Basak, Vaishnavi Ranganathan, Seetharam Narasimhan and Swarup Bhunia

***Abstract*— High Intensity Focused Ultrasound (HIFU) is emerging as an accurate, noninvasive method for ablation of certain primary and metastatic tumors. Typically, ablation is performed with an external therapeutic transducer. However, external HIFU treatment suffers from limitations of low therapeutic efficiency for ablation of tumors, deep in internal organs such as liver, kidney and brain. Interstitial HIFU through an internal transducer, implanted locally near the organ of interest, could alleviate some of these limitations. Furthermore, it can be attractive for point-of-care (POC) treatment. In this paper, we propose the design of a dual-functional implantable assembly for image-guided HIFU treatment of anomalous growth. It is realized by effective integration of a central HIFU array with two ultrasonic imaging arrays for high-resolution online monitoring and efficient treatment. We explore the design space for the implant and identify the major design parameters including the power requirement. Using a widely used simulation platform, we show that the proposed implant, besides providing a potential POC solution, achieves a better therapeutic performance for certain tumor positions in internal organs, than the extracorporeal HIFU treatment.**

I. Introduction

High Intensity Focused Ultrasound (HIFU) has emerged as a precise medical procedure to treat anomalous growth. Compared to conventional cancer treatment modalities such as open surgery, radio and chemo-therapy, HIFU shows great promise in treating many forms of cancer due to its non-invasiveness, reduced toxicity, better focusability, and fewer complications post-treatment [1]. Fig. 1(a) illustrates a general mode of HIFU operation, where a concave transducer is used to focus the beam at a tumor, surrounded by healthy tissue. In current medical practice, primarily extracorporeal HIFU is used to target and ablate tumors in organs that are readily accessible through an acoustic window on the skin. Usually, concave self-focusing transducers or linear transducers with acoustic lens are used for providing the HIFU beam. Phased arrays of $\geq$ 128 elements are also used to allow for rapid electrical steering of the HIFU focus through the diseased tissue and achieve a greater accuracy in the focal geometry.

External HIFU treatment, however has its limitations, and associated risks, which may lead to adverse outcomes [1].
1) Tumors that are deep within interstitial organs ($>$ 8 cm) would be difficult to treat as the acoustic energy reduces greatly due to effects such as frequency dependent attenuation and reflection at tissue interfaces. Refraction artifacts can result in energy deposition in soft tissues adjacent to the desired target. Phase aberrations due to non-homogeneity, leads to distortion in the beam localization at the focus.
2) Bones and gas (as in bowel) strongly oppose the penetration of ultrasound due to high reflection and absorption of ultrasound energy. Brain tumors and certain liver parenchymas, are difficult to treat with external HIFU due to the presence of the skull and the rib cages in the propagation path.
3) The step of preplanning under image guidance often takes long time to achieve the desired focal accuracy. This is primarily due to the variability in the acoustic parameters for tissues, error in the imaging feedback for guidance etc. Misregistration, due to respiratory or bulk patient movement, may also be problematic in external HIFU.

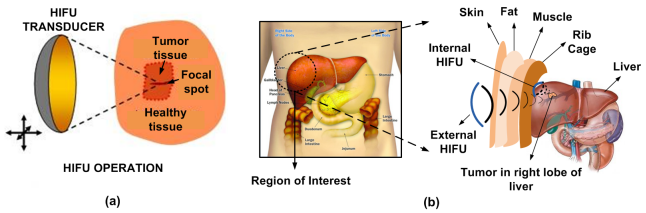

Fig. 1. (a) A common mode of HIFU operation; (b) HIFU treatment of a tumor in liver using external or internal therapeutic assembly.

To address these limitations of external HIFU, we propose an implantable dual-functional device for monitoring and treatment of abnormal growth. The comparative situation is illustrated in Fig. 1(b). The HIFU device is integrated with a high resolution, automated implantable ultrasonic assembly, for monitoring and timely detection of recurrence of malignancy [2]. We consider liver as the organ of interest in the case study. It has deep internal regions e.g. near diaphragm and around gall bladder, which are difficult to access with external therapeutic ultrasound. Besides, the ribs significantly attenuate the energy towards the target area and absorb/reflect the incident energy, leading to skin burns. They also cause phase aberrations leading to beam distortion, which prevents the desired temperature rise at the target area. Often, partial removal of ribs, through surgery is necessary to avoid this problem. Segmented arrays also, suffer from proper focusability. Finally, accuracy of HIFU suffers from the non-homogeneity of tissues (skin, fat, muscle, bones) in the propagation medium. Hence, for treatment of tumors in internal organs like liver, in presence of non-homogeneity and limited acoustic windows, internal HIFU, placed close to the tissues of interest is an attractive option.

The major contributions of the paper are as follows:
1) It proposes a novel, dual-functional implantable ultrasonic

The authors belong to the Electrical Engineering and Computer Science Department, Case Western Reserve University, Cleveland, OH, USA- 44106. Email: (axb594, vxn55, sxn124, skb21)@case.edu.

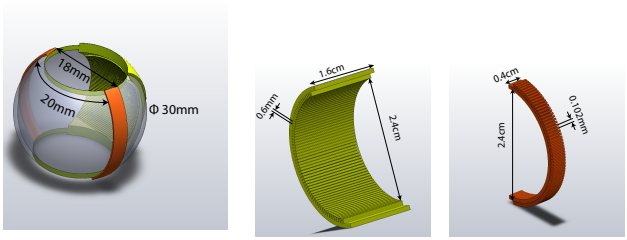

(a) (b) (c)

Fig. 2. (a) Implantable assembly; (b) HIFU array; (c) imaging array.

assembly for efficient treatment of anomalous growth. The imaging assembly is capable of providing high resolution image of a susceptible region.The treatment is done through localized interstitial HIFU under ultrasound image guidance. Such a device can provide a long-term point-of-care therapeutic solution and can be inserted in a region of interest during surgery - e.g. during resection of a primary tumor.
2) It explores the design space and identifies the major design issues, including power requirements for the implant.
3) It evaluates the effectiveness of interstitial HIFU and compares it to currently practised external HIFU system for ablation of tumors in deep, internal organs like liver. It shows that internal HIFU provides higher therapeutic efficiency and reduced probability of damage to benign cells.

II. Proposed System

The proposed dual-functional implantable therapeutic unit builds on the implantable imaging system we have investigated before [2]. Once the internal imager detects an anomaly and sets an alert and further clinical tests (MRI scans, biopsy etc.) confirm the presence of tumor, the internal HIFU transducer, in the assembly could potentially be used to ablate the desired tumor under the imaging feedback guidance. The parameters for therapy namely the phasing delays, voltage levels etc. would be applied by the clinician, through external RF control signalling.

1) ***Transducer Selection****:* As described in [2], the internal imaging arrays are convex curvilinear arrays, composed of soft PZT-5H or Capacitive Micro-machined arrays. For better focusing performance, concave curvilinear arrays would be used as HIFU transducers. As early detection of tumor growth, is still the primary function of such an assembly, we choose different materials for imaging (PZT-5H) and therapeutics (hard PZT's like PZT-4 or 8) respectively. The HIFU transducers should be able to cover the range of scanning (the 3D volume) of the imaging assembly.

2) ***Array Positions****:* To incorporate concave arrays, we need to extend the design in [2], to a sphere of radius 1.5 cm, with interposed convex imaging and HIFU concave arrays. To increase the net HIFU aperture area for lesser surface intensity, we go with one single concave HIFU array, flanked by two convex imaging arrays on the sides, instead of other combinations, as shown in Fig. 2(a).

3) ***Array Parameters****:* To prevent overlap of the array surfaces near the vertices, the arrays (imaging and HIFU) extend up to 0.3 cm from the vertices on either sides. The width of the HIFU arrays are fixed to allow unobstructed passage of the therapeutic beam. These 2 arrays are separately shown in Fig. 2b and c. Considering trade offs between peak power and therapeutic efficiency, the number of beam forming channels for a HIFU array is limited to 64. As described in the subsequent section, 3 MHz is chosen as the internal HIFU frequency. For our HIFU array, this corresponds to a pitch of 0.6 mm = 1.15λ. A pitch $>$ than Nyquist rate would correspond to grating lobes, but in general in concave phased arrays, the grating lobes are minimized [5].

4) ***Beam Steering****:* With our HIFU array pitch, the focus can be steered in the lateral direction up to $\sim 20°$ on either side of the acoustic axis. Thus, without any mechanical movement of the assembly, each HIFU array would be able to ablate a tumor in a unit therapeutic volume, determined by allowable steering. Hence, coarse grained rotation is performed mechanically to fix acoustic axis and fine grained rotation by steering on either sides of the focal volume.

A. HIFU Operation Flow

Fig. 3 is an illustration of typical interstitial HIFU flow with the different sequential steps as follows-
1) **Alignment** - Align the HIFU array, with tumor center from prior localization information (internal imaging).
2) **Preplanning** - Parameters are set to achieve beam localization at sub-therapeutic intensities, after imaging feedback.
3) **Therapy** - With the set parameters, ablation phase, for a unit volume is conducted at therapeutic power levels.
4) **Imaging Feedback** - Thermometric feedback from the internal imager, regarding the focal temperature rise.
5) **Further Iterations** - Further therapy is conducted according to imaging feedback results, tumor dimensions etc.

B. Power Analysis

Out of the dual functionalities, HIFU is the critical mode for power and energy analysis. As a rough estimate for the HIFU power/energy requirements, taking the typical values of I_{spta} at the focus, worst case focal gain, electro-acoustic efficiency, the peak electrical power demand is $\sim 200W$. For a unit therapeutic volume ablation, the energy required is $\sim 5KJ$. By similar calculations for preplanning, the peak power is $\sim 30W$ and energy being $\sim 300J$. Neglecting the power for image guidance and micro-motors compared to ablation levels, the total energy for HIFU is $\sim 5.3KJ$. The

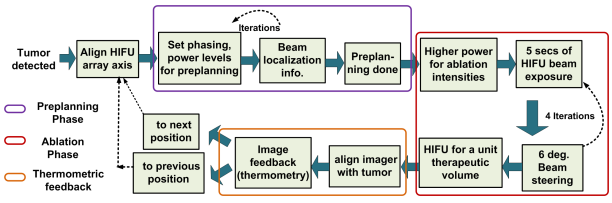

Fig. 3. Flow of operations within the implant during treatment of an anomalous growth.

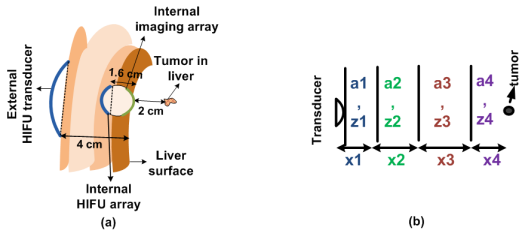

Fig. 4. (a) Distance considerations used in simulation framework; (b) illustration of non-homogeneity of intervening medium.

excitation voltage and peak current for the HIFU transducers are $\sim 30V$ and $\sim 7A$ respectively .

Regarding the power source, we consider an implantable battery, with capacity 410 mAh [6]. With a loading voltage drop of 0.8 V, the battery voltage is $\sim$ 2.8 V. For an excitation voltage of $\sim 30V$, we proceed with a series connection of 3 such batteries (implanted subcutaneously with wired connection) and a 6 stage Dickson charge pump (simulated output voltage of 28.8 V). The energy, available from the power source is $\sim 12.4KJ$. For an operating time of $\sim 50sec$, the peak current available from the source would be $\sim 30A$, much greater than required peak current.

III. Simulation Results

A. Simulation Framework

We compare the therapeutic performances of an external and an internal HIFU assembly for tumor ablation at various depths from the liver surface. Optimal choice of therapeutic frequency is application specific, ranging from $\sim$ 0.5 MHz for deep regions, and $\sim$ 6-8 MHz for superficial transrectal applications for prostrate. It is observed that therapeutic frequencies of $\sim$ 1 MHz is ideal for heat deposition in all intermediate cases [1]. As the possible focal positions for external HIFU varies from $\sim$ 4 cm to $\sim$ 9.5 cm and beyond, the probable external therapeutic frequency would be 1 MHz. Field II allows for the simulation of concave transducers, with a circular aperture, a common topology for HIFU transducers.The diameter of the external concave transducer was constrained to 6 cm. The aperture of the internal transducer is $2.4 \times 1.62cm^2$, equivalent in surface area to that of a concave transducer of radius 1.15 cm. For comparative studies, the aperture radius of interstitial transducer is 1.15 cm and that of the external HIFU transducer is varied between 2, 2.5 and 3 cm depending on the available acoustic windows between $10 - 30cm^2$. 5 focal positions from 1-5 cm from the liver surface were taken into consideration, corresponding to a distance of $\sim$ 2.6-6.6 cm from the internal concave HIFU array as shown in Fig. 4(a). Non-homogeneity in the external scenario has been incorporated, as described in the subsequent section. For all comparative simulations of HIFU performance, the excitation voltage was set in order to achieve a spatial-peak temporal average (I_{spta}) intensity of 1 KW/cm^2 at the focal point (tumor center). Analysis is restricted to the azimuthal plane only. The therapeutic metrics analyzed are as follows:

1) **Focal Area:** The area around the focal point, beyond which the intensity falls 3dB below the focal point intensity.
2) **Surface Intensity:** The average acoustic intensity along the surface of the transducer. Surface intensities are usually high in HIFU, which often leads to skin burns, blisters etc.
3) **Focal Gain:** The ratio of the mean intensity at the focal spot to the average surface intensity. It is a measure of the efficiency of the HIFU assembly in tumor ablation.
4) **Distortion Index (DI):** DI is calculated from the average intensity inside a particular spatial boundary and outside the focal area, normalized with respect to the focal point intensity. This roll off is important for monitoring the safety of the organ cells, nerve cells etc. around the tumor.

For HIFU operation, to select the therapeutic frequency, for a fixed aperture, there is a tradeoff between accuracy of focusing at the focus and the losses due to attenuation. For extracorporeal HIFU ablation of liver tumors, mainly the attenuation effect predominates after a certain depth and hence a relatively low frequency of 1 MHz is chosen. The above mentioned trade off plays a significant role in the selection of our internal HIFU frequency. For 4 possible frequencies of 1-4 MHz, the internal therapeutic performance was quantified by calculation of the above described metrics for the different depths (1-5 cm). An equal metric weighted cost function was averaged over the 5 depths for each frequency. In our case, the lowest value was obtained at 3 MHz, and hence selected as the interstitial HIFU frequency.

1) Non-Homogeneity Using Field II: Non-homogeneity is especially prominent in external HIFU scenario. Field II does not possess features to specify different attenuation coefficients at different depths for field calculation. We decided to use a weighted averaging method to approxi-

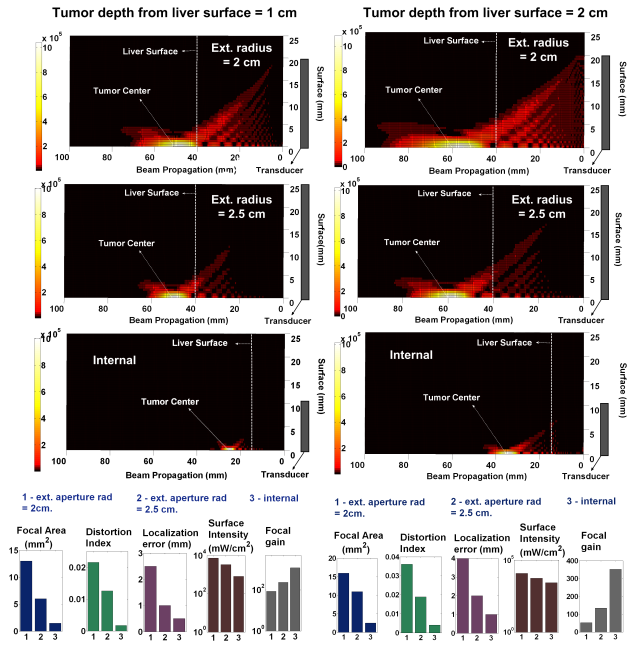

Fig. 5. Internal/external HIFU spatial intensity maps, illustrating and quantifying (from metrics values) the better internal therapeutic performance.

mately calculate the equivalent attenuation coefficient for field points, at various depths along the propagation path. Attenuation of ultrasound usually comprises of absorption ($\sim$70%) and diffuse scattering of the beam ($\sim$30%). The effect of interface reflections is clubbed together with the attenuation losses into an equivalent attenuation value for a point, considering a linear model of propagation (Field II is based on the linear models). For a typical external case, as in Fig. 4(b), let the thickness, attenuation coefficients and impedances of the 4 layers be xi,ai, and zi, i being the layer number. Let the fractional losses due to reflection at the interfaces of 1 and 2, 2 and 3, 3 and 4 be L_{12}, L_{23} and L_{34} respectively. If the acoustic pressure at the transducer surface is P and the frequency is 1 MHz, then the total losses T_L, till the field point, is $T_L = P * exp^{-a1*x1} * L_{12} * exp^{-a2*x2} * L_{23} * exp^{-a3*x3} * L_{34} * exp^{-a4*x4}$. The total losses may also be written in the form an equivalent attenuation coefficient a as $T_L = P * exp^{-a*(x1+x2+x3+x4)}$. Equating them, we obtain the net attenuation coefficient to be incorporated into Field II. The acoustic parameters and thicknesses values are obtained from [7]. In an actual scenario, there are non-linear effects affecting the beam propagation, leading to greater losses. Hence our approach is conservative.

B. Therapeutic Phase

For the ablation procedure, with the set preplanning parameters, the excitation voltage is increased so as to obtain I_{spta} between 500-10000 W/cm^2 at the focal point. In our simulations, I_{spta} is taken as 1 KW/cm^2.

The intensity maps for internal and external HIFU beams, with tumor centers at a distance of 1 cm and 2 cm respectively, from the liver surface are shown in Fig. 5, along with the corresponding metrics. All the maps are shown up to 25 mm along the surface for comparison. As observed from the figure, the focusability in terms of roll off around the focus and the corresponding focal spot dimensions is much better in the internal case as compared to the external HIFU performance, for both scenarios. Besides, the intermediate medium between the focal point and the transducer surface, in general has a lower value of intensity distribution for the internal therapy, as seen from the color coded maps with little variation in the surface intensities for the 2 maps.

Fig. 6 shows the variation of the different HIFU metrics, within the internal imaging scan range (1-5 cm), for internal and the 3 possible external HIFU apertures. We observe from the figure, that both the -3 dB focal area and the distortion index are much lower for the internal HIFU mode at almost all depths as compared to the 3 external apertures($\sim$ 3-10X times lower as compared to external HIFU, for lower depths). Finally, internal HIFU fares better than external HIFU modes in both metrics of surface intensity (low) and focal gain (high), at lower external apertures (2cm and 2.5 cm radius) at lower depths of focus ($< 4cm$), with the performance of the higher aperture external case slightly better than the internal. From the trends, we can infer that in the real scenario, HIFU ablation performance would be better for our interstitial HIFU assembly for most tumor positions in the right lobe of liver, with the probable exceptions of external HIFU through large acoustic windows (e.g. intercostal spaces between 6th and 7th ribs etc.) for ablation of distant tumors.

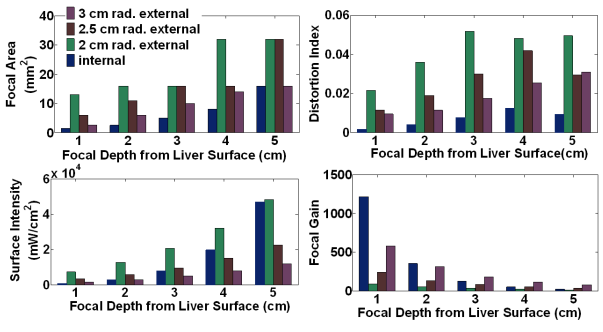

Fig. 6. Comparison of internal/external HIFU therapeutic performance.

IV. Conclusion

We have presented the design and analysis of a novel dual functional implantable ultrasound imaging and therapeutic assembly for monitoring and image-guided ablation of tumors. The implant can be inserted in a patient during surgery (e.g. resection of a primary tumor) to monitor a vulnerable site and treat a malignant growth (e.g. a recurrence). The system integrates ultrasound imaging arrays for diagnostic and a HIFU transducer for therapeutic purpose. Use of ultrasound technology, which is safe, low-cost, and can be easily miniaturized, helps us achieve a long-term, affordable, point-of-care solution for both diagnostics and treatment. Furthermore, based on extensive analysis using a widely-used ultrasound simulator, we show that the proposed interstitial HIFU assembly can achieve better therapeutic efficiency than extracorporeal HIFU for tumors in deep internal organs like the liver. In addition to liver and other internal organs (e.g. gall bladder, pancreas, which suffer from reduced ultrasonic accessibility), the proposed implant is promising for screening and treatment of different forms of brain cancers, such as glioma. Future work would focus on experimental validation of the proposed device and application to various forms of cancer.

References

[1] Y. F. Zhou, "High Intensity focused ultrasound in clinical tumor ablation," *World Journal of Clinical Oncology*, vol. 2(1), pp. 8-27, 2011.

[2] A. Basak, S. Narasimhan, and S. Bhunia, "Low-power implantable ultrasound imager for online monitoring of tumor growth," *Proc. IEEE EMBC Annual Conference*, pp. 2858-2861, Sept 2011.

[3] E. K. Outwater, "Imaging of the Liver for Hepatocellular Cancer," *Cancer Control*, vol. 17, no. 2, pp. 72-82, 2010.

[4] E. S. Ebinni, C. Simon, H. Lee, and W. Choi, "Self-guided ultrasound phased arrays for noninvasive surgery," *Proc. IEEE Ultrasonics Symposium*, vol. 2, pp. 1427-30, Oct. 1999.

[5] Y. Wan and E. S. Ebinni, "Imaging with Concave Large-Aperture Therapeutic Ultrasound Arrays Using Conventional Synthetic-Aperture Beamforming," *IEEE Trans Ultrason Ferroelectr Freq Control.*, vol. 55(8), pp. 1705-1718, Aug. 2008.

[6] "Rechargeable Lithium-ion Batteries QL00370B," *http://www.quallion.com/new-pdf/QL0370B.pdf*.

[7] T. L. Szabo, "Diagnostic Ultrasound Imaging Inside Out," *Academic Press*, 2004.